Design and Testing of a Small Inductive Pulsed Plasma Thruster

IEPC-2015-50／ISTS-2015-b-50

Presented at Joint Conference of the 30th International Symposium on Space Technology and Science 34th International Electric Propulsion Conference and 6th Nano-satellite Symposium, Hyogo-Kobe, Japan July 4 – 10, 2015

Adam K. Martin[1], Alexandra Dominguez[2], Richard H. Eskridge[3], Kurt A. Polzin[4], Daniel P. Riley[5]
NASA – George C. Marshall Space Flight Center, Huntsville AL 35812, USA

Kevin A. Perdue[6]
Sun Hydraulics, Sarasota FL 34243, USA

The design and testing of a small inductive pulsed plasma thruster (IPPT) is described. The device was built as a test-bed for the pulsed gas-valves and solid-state switches required for a thruster of this kind, and was designed to be modular to facilitate modification. The thruster in its present configuration consists of a multi-turn, spiral-wound acceleration coil (270 mm o.d., 100 mm i.d.) driven by a 10 μF capacitor and switched with a high-voltage thyristor, a propellant delivery system including a fast pulsed gas-valve, and a glow-discharge pre-ionizer circuit. The acceleration coil circuit may be operated at voltages up to 4 kV (the thyristor limit is 4.5 kV) and the thruster operated at cyclic-rates up to 30 Hz. Initial testing of the thruster, both bench-top and in-vacuum, has been performed. Cyclic operation of the complete device was demonstrated (at 2 Hz), and a number of valuable insights pertaining to the design of these devices have been gained.

Nomenclature

f_C	=	cyclic rate (Hz)
FRD	=	Fast Recovery Diode
IPPT	=	Inductive Pulsed Plasma Thruster
I_{bit}	=	impulse bit (kg-m/s)
I_{SP}	=	specific impulse (s)
L_C	=	coil inductance (nH)
L_{circ}	=	circuit inductance (nH)
L_{eff}	=	effective inductance of coil (nH)
L_0	=	external inductance (nH)
m_{bit}	=	propellant mass bit (μg)
PIT	=	Pulsed Inductive Thruster
Q_{rr}	=	reverse recovery charge (mC)
P_{Jet}	=	jet power (kW)
R	=	circuit resistance (mς)
V_{Ch}	=	capacitor charge voltage (V, kV)
v_e	=	exhaust velocity (m/s)

[1] Aerospace Technologist, Propulsion Systems Department, adam.k.martin@nasa.gov
[2] Aerospace Flight Systems Engineer, Spacecraft and Vehicle Systems Department, alexandra.dominguez@nasa.gov
[3] Propulsion Systems Engineer, Propulsion Systems Department, richard.h.eskridge@nasa.gov
[4] Propulsion Research Scientist, Propulsion Systems Department, kurt.a.polzin@nasa.gov
[5] Aerospace Engineer, Propulsion Systems Department, daniel.p.riley@nasa.gov
[6] R&D Engineer, kaperdue78@aol.com

I. Introduction

THE Inductive Pulsed Plasma Thruster (IPPT) is a class of electric thruster in which energy stored in a capacitor is rapidly discharged through a coil, inducing magnetic fields that drive currents in a plasma and accelerate it to produce thrust[1]. One of the more famous embodiments of this class is the large Pulsed Inductive Thruster (PIT)[2]. The potential benefits of the concept are: long operational life-time due to the absence of high-current electrodes, the ability to run on readily storable molecular propellants such as ammonia, and an I_{SP} that is independent of jet-power, P_{Jet}. This last feature may make the IPPT particularly suitable to certain classes of deep-space missions[3].

An IPPT typically consists of a spiral-wound acceleration coil, which is connected to a discharge circuit consisting of a capacitor-bank and a switch. A pulsed gas-valve injects gaseous propellant over the face of the coil, and then the switch is closed, discharging the capacitor through the coil. The fast-rising current pulse through the coil ionizes the propellant, which accelerates away from the coil due to the ***JxB*** (Lorentz) body force applied to the plasma by the interaction of the magnetic field produced by the coil and the current induced in the plasma. A pre-ionizer circuit may also be used to partially ionize the gas just prior to the discharge of the capacitor, so as to improve the coupling. An individual pulse, as described above, is repeated at some cyclic rate, f_C, producing a steady thrust. The I_{SP} of the device is set by the characteristics of an individual discharge: the propellant mass bit, m_{bit}, and impulse bit, $I_{bit} = m_{bit} \langle v_e \rangle$, where $\langle v_e \rangle$ is the average exhaust velocity of the propellant. The thrust is then given by $T = f_C I_{bit}$ and the jet power is given by $P_{Jet} = f_C I_{bit}^2 / (2 m_{bit})$.

A small thruster with a nominal P_{Jet} of a few kW has been built to demonstrate operation of an integrated solid-state switched IPPT. The goal of the effort was to build a device that could be tested in cyclic mode on a thrust-stand, and which could augment the existing data set for these devices[4]. In addition, the thruster was designed to serve as a test-bed for solid state switching circuitry and pulsed gas valves. The modular design of the device allows for a variety of configurations to be tested. A more detailed explanation of the design rationale and more detailed descriptions of the some of the thruster's sub-systems are given elsewhere[4].

II. Design and Fabrication of the Thruster

The acceleration coil circuit consists of the coil, the capacitor bank, and the switch assembly. A schematic of this circuit is shown in Fig. 1. In addition to these three subsystems, there is a propellant delivery system, and a pre-ionizer. These components are described in greater detail in the following sub-sections.

The thruster is built on a framework of two 12.7 mm (1/2") thick Lexan plates, adjoined by four 15.9 mm (5/8") diameter fiberglass threaded rods. The partially assembled device with the acceleration coil circuit is shown in Fig. 2. This is the configuration that was used for the bench-top testing described in section III.A.

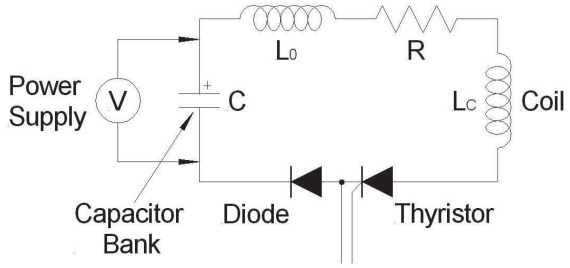

Figure 1. Schematic of the acceleration coil circuit

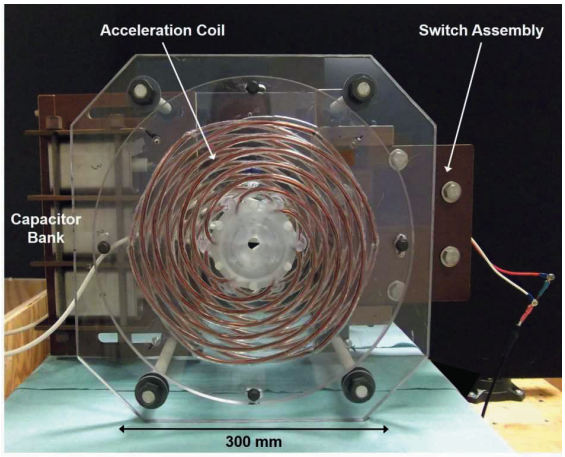

Figure 2. Partially assembled IPPT showing the coil, capacitor bank, and switch assembly.

A. Acceleration Coil

The acceleration coil (see Fig. 2) has an outer diameter of 270 mm and an inner diameter of 100 mm. It was wound on a lexan coil-form and consists of six leads (connected in parallel) that are clocked around the form at 608 intervals. The leads are No. 10 magnet wire with

enamel insulation and are further insulated with Teflon heat-shrink tubing. The leads are laid in spiral-shaped grooves that were CNC-machined in the coil-form. Each lead begins on the top side of the coil form at the inner radius, makes a one-turn spiral to the outer-radius, threads through to the bottom of the coil form, and spirals back to the inner-radius. The path described by the leads on each side of the coil-form is an Archimedes-spiral ($r = a + b\upsilon$); each lead makes two complete turns around the axis of the device.

For additional high-voltage insulation, the coil was potted with Momentive RTV-560, a high-voltage silicone insulation compound. The coil face was covered with an annular disk to provide additional insulation between the plasma and the coil and to serve as a suitable refractory plasma-facing surface. The disk, a Mylar sheet, was covered with a layer of alumina felt that was brushed with an emulsion of silica particles in water (called "water-glass"); when dried, it sets up as a matte, non-porous surface.

B. Capacitor Bank

The energy for each discharge is stored in 10 μF capacitors (nominal capacitance), which are oil-filled and rated for use in vacuum. They have a voltage rating of 7.5 kV and a series inductance of not more than 20 nH. Up to three such capacitors can be mounted on a phenolic bracket connected to the thruster frame. To date and for the work described in this paper, only one capacitor has been used. Its capacitance, measured with a Fluke Model 87 V meter, is 9.88 μF. Brass spheres with tapped 10-24 holes on milled-flats were screwed on to the capacitor terminals to serve as the terminations. The high-voltage cables used to wire the circuit were fastened to these spheres.

C. Switch Assembly

The capacitor bank is switched with a Dynex PT85QWx45 pulse-power thyristor, which is configured in a "hockey-puck" package. It is rated for a maximum hold-off voltage of 4.5 kV, an RMS current of 1.2 kA, a maximum surge current of 30 kA, and a maximum dI/dt of 22 kA/μs. The acceleration coil circuit was designed so that the maximum initial current rise rate would stay within the dI/dt limits of the switch. The thyristor is turned on with a gate-circuit that supplies an initial fast-rising 1.7 A pulse to the gate, with an optional 400 mA "back-porch" plateau current after the initial pulse (recommended by the manufacturer). The signal from the gate circuit is applied across the gate and cathode terminals of the thyristor; as the circuit is battery-powered and fiber-optically triggered, it is otherwise electrically isolated.

Ideally for a thruster of this kind, the current is shut off at the first zero-crossing of the current, after the first half-cycle of the discharge. This can in principle be accomplished with a fast recovery diode (FRD) placed in series with the thyristor. The FRD recommended for use with the PT85QWx45 thyristor is the DSF21545SV (also in the "hockey-puck" package and also made by Dynex), with a maximum current rating of 20 kA. Although this is the fastest FRD that could be obtained and which could accommodate the required current, its recovery time of 7 μs and reverse recovery charge, Q_{rr}, are still likely inadequate for this application. None-the-less, we tried using it anyway to gain some experience with these devices.

The thyristor and diode are stacked together in series and held in a clamp assembly (shown in Fig. 3) which provides the 40 kN (8,990 lbf) clamping force required for proper operation of the switch. The two components are held in compression between 12.7 mm (1/2") thick stainless-steel discs inserted into 25.4 mm (1") thick phenolic blocks. The blocks are drawn together with six 12.7 mm (1/2-13) stainless-steel bolts, torqued to 8.47 N-m (75 in-lbs). Bellville washers, with a flat-load of 6.56 kN (1,475 lbf) were used with the bolts to maintain the desired compressive load. Electrical connection to the thyristor and diode were made to 1 mm (0.040") thick copper tabs that were held in the stack by compression. To minimize contact resistance, Cool-Amp silvering powder was applied to the tabs. Additionally, 0.25 mm (0.01") thick silver gaskets were placed between the thyristor and diode, and between both of those components and the copper tabs.

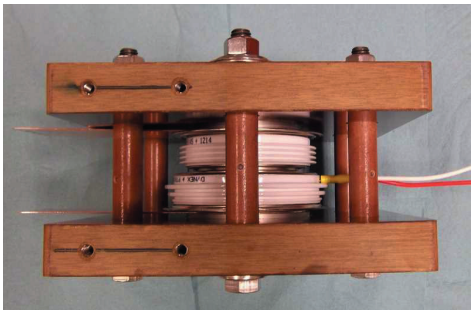

a.)

b.)

Figure 3. Switch Assembly: a.) side view b.) oblique view, showing the copper tabs used for connecting the HV cables.

D. Propellant Delivery System

The propellant is injected over the coil face using a fast pulsed gas valve, shown in Fig. 4. A Parker Pneutronics 12 V solenoid valve was modified to serve this purpose. The valve body was modified to eliminate the dead-space down-stream of the outlet, and a thin, drawn glass tube was glued into the inlet with Torr-Seal creating an orifice that limits inflow into the internal plenum. When the poppet is lifted, the plenum is rapidly exhausted through the outlet, but is only slowly replenished through the inlets limiting orifice. The valve was soldered to a brass KF-16 flange, for mounting on a test chamber for detailed characterization, prior to installation in the thruster. To open the valve quickly, the solenoid is over-driven with a 320 V pulse, supplied by a driver-circuit that can operate at cyclic-rates up to 30 Hz. The opening time of the poppet was measured to be 300 μs.

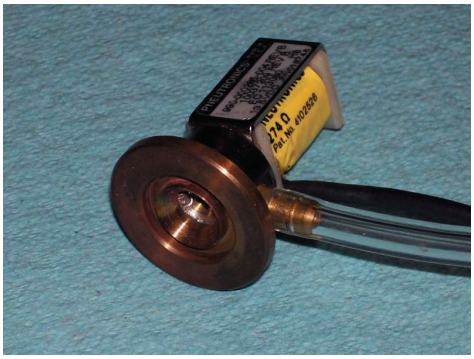

Figure 4. Pulsed gas valve.

The valve is contained in a Lexan housing that mounts to the coil form, in-line with the thrust-axis. The gas flow from the valve, initially axial, is redirected to a radial flow over the coil face by a stainless-steel flow-diverter, which also serves as the inner electrode of the pre-ionizer system. The valve housing assembly is shown in Fig. 5.

The valve can be supplied with gas from a small reservoir (run-tank), mounted directly on the thruster to avoid pressure-drops in the propellant line that could hinder replenishment of the valve plenum, should that be a problem. The run-tank is equipped with isolation valves, a pressure regulator, transducers for monitoring the pressure upstream of the limiting orifice and in the run-tank, and a thermistor for measuring the run-tank temperature. The volume of the run tank and manifold is approximately 140 ml. The mass-flow to the thruster can be determined from the temperature and the change in pressure in the run-tank during a gas pulse.

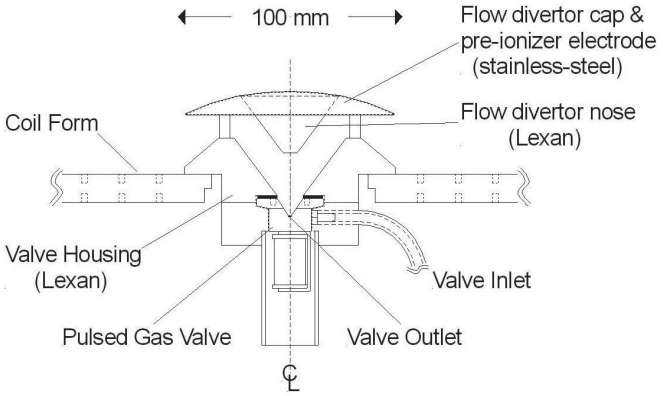

Figure 5. Plan-view of the pulsed gas-valve and housing.

E. Pre-ionizer

A DC glow-discharge pre-ionizer, shown in Fig. 6, is used to provide initial ionization of the propellant gas. A 0.3 μF capacitor, charged to 4.1 kV (stored energy of 2.5 J), is connected across two electrodes, that bound the coil-face. The inner electrode is also the flow-diverter described in section II.D.; the outer electrode consists of four polished stainless-steel tubes on the coil periphery. When propellant is puffed from the valve and flows out over the coil face, it bridges the two electrodes, discharging the capacitor, and ionizing the gas. The capacitor connects to the electrodes through a 2.9 kς current-limiting resistor. The pre-ionizer circuit is isolated and battery-powered.

The outer electrodes are supported by four Lexan posts which also hold down the alumina disk. They also support a Mylar propellant-cuff that helps to confine the gas to the region over

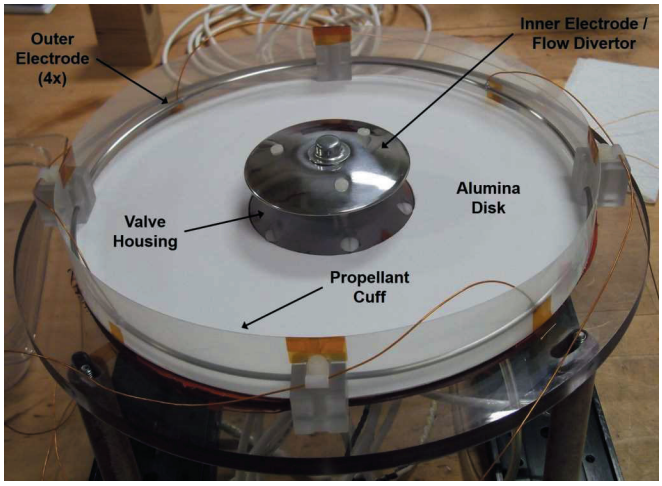

Figure 6. The coil-face with alumina disk, pre-ionizer electrodes and valve holder.

the coil. The posts and propellant-cuff will eventually be coated with alumina felt or a spray-on boron-nitride coating.

F. Electrical Connections and Insulation

Electrical connections between the coil, capacitor bank, and switch assembly, are made with stranded, silicone-rubber insulated high-voltage cables (12 AWG) rated to 30 kV. The cable ends connected to the coil were soldered to the coil leads and insulated with heat-shrink tubing; those connected to the capacitor and switch-assembly were furnished with ring-lugs, that were crimped and soldered to the cables. All remaining exposed metal surfaces were insulated with several layers of RTV 560 or liquid-tape.

III. Experimental Results

A. Bench-top Testing

Prior to final assembly and insulation of the thruster, bench-top testing of the acceleration-coil circuit was carried out to measure circuit parameters, and to test the components at high voltage. These measurements are described in the subsequent two sections. Additional measurements, described elsewhere[5], were performed using alternate diodes, including a SiC diode, to determine current clamping characteristics of those devices. For the tests described in this section, the thruster was fired only in single-pulse mode, not repetitively. The capacitor bank was charged with a Bertan model 205-20R high-voltage power-supply.

1. Measurement of the Coil Inductance and Stroke-Length

A series of tests were conducted to determine the inductance of the coil, L_C, the external (stray) inductance of the circuit, L_E, and the characteristic de-coupling length of the coil (also called the stroke-length), z_S. A copper disk with dimensions 102 mm i.d., 292 mm o.d., and 1.6 mm thick, was used to mimic the effect of the plasma. This disk (sometimes referred to as a 'dummy plasma') was mounted to an optics-rail, aligned along the axis of the thruster. The thruster was set on a wooden platform that was set on a wooden table, so that the center of the coil was at least two coil diameters away from any metal objects not associated with the thruster itself. The copper disk was suspended at the end of a phenolic boom held above the table on a phenolic stanchion, so that it was likewise far away from any extraneous pieces of metal. The experimental configuration is shown in Fig. 7. For this series of tests, the diode was removed so that the circuit would ring freely. It was replaced with a 25.4 mm thick aluminum disk of approximately the same diameter as the diode, so that the inductance of the switch-assembly would be about the same as with the diode.

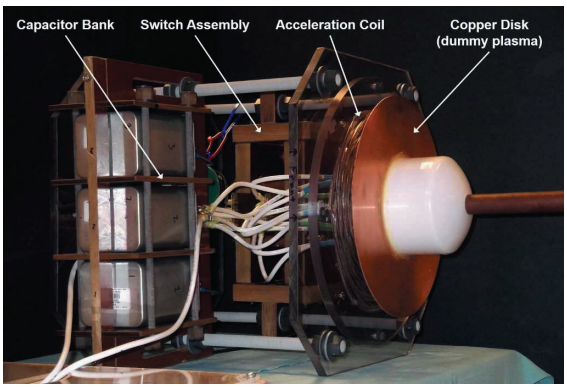

Figure 7. Arrangement of the thruster and the dummy plasma for measurement of the coil inductance and stroke-length.

Starting at an axial displacement of z = 2.5 mm from the coil-face, the disk was stepped out to several axial locations. At each location, with the capacitor charged to a value $V_{Ch} \sim 250$ V, the thyristor was triggered and the resulting current waveform recorded. The current was measured with a Pearson current probe (Mod. No. 4418) and the voltage on the capacitor was measured with a Tektronix P5210 high-voltage probe (in ground-referenced mode); the data was recorded on a Tektronix TDS 3052 oscilloscope.

The total inductance of the circuit, L_{circ}, can be determined from the measured current waveform, as can the circuit resistance, R. This inductance includes both the effective inductance of the coil in the presence of the copper disk, L_{eff}, as well as the external inductance of the circuit, L_0; $L_{circ} = L_0 + L_{eff}$. For each axial position, the waveform was fitted (using IGOR Pro, Wavemetrics, Portland, OR) with a damped sine function, characteristic of an RLC circuit. As C is known, R and L_{circ} may be calculated from the resulting fit. At the low charge voltages used, R was relatively high and the circuit rang out in about two cycles. In all cases, the fitting was performed over about 1.2 cycles. The resulting values of L_{circ} vs. the axial position of the copper disk are shown in Fig. 8.

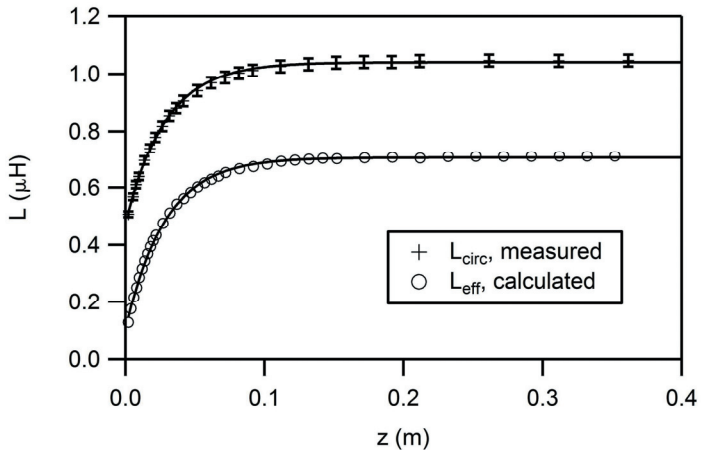

Figure 8. Measured circuit inductance, L_{circ}, and calculated effective coil inductance, L_{eff}, vs. axial displacement of the copper disk. The error bars on L_{circ} range from ±10 nH to ±20 nH. The assumed error bars for L_{eff} (not shown) are ±10 nH. The solid lines are fits to the points using Eq. 1.

The effective inductance of the coil itself, L_{eff}, in the presence of the copper disk and independent of any external inductance due to the overall circuit, was calculated using QuickField v5.6 (Tera Analysis, Toronto, Canada), a 2-D axisymmetric magnetic field solver. This calculation was done using a method that was developed for calculating the inductance of IPPT coils[6]. The results of these calculations are also shown in Fig. 7. The asymptotic value of L_{eff}, when the copper disk is far enough away from the coil as to be electromagnetically decoupled, is the unloaded coil inductance, L_C.

Also shown in Fig. 8 is a fit to L_{eff} using the function shown in Eq. 1, which has been found to describe IPPT acceleration coils well[7]. In Eq. 1, k_0 is a constant, equivalent to a transformer coupling constant, and L_∞ is the asymptotic value of L as z approaches infinity. From this fit, L_C (= L_∞), z_S, and k_0 are determined. Eq. 1 was also used to fit the data for L_{circ} in order to determine the total circuit inductance with an unloaded coil (in this case, k_0 is unimportant as it includes the effect of L_0).

$$L(z) = L_\infty \left(1 - k_0^2\, e^{-2(z/z_S)}\right) \tag{1}$$

The fitting parameters for these two curves are summarized in Table 1. The reduced goodness-of-fit parameter, $\xi^2 / \nu = \xi^2 / (N - p - 1)$, is also shown, where N is the number of points fit to and p is the number of independent fitting parameters (p = 3); $\xi^2 / \nu < 1$ for both curves, indicating a good fit.

The difference in the value of L_∞ between L_{circ} and L_{eff} may be taken as the external inductance of the circuit: L_0 = (336 ± 8) nH. The stroke-length of the coil is the same for both curves to within their calculated uncertainties; z_S = (57 ± 3) mm.

Table 1. Fitting parameters used for Fig. 8.

	Quantity fit to:	
Fitting Parameter:	L_{eff}	L_{circ}
L_∞ **(nH)**	705 ± 3	1,041 ± 7
z_S **(mm)**	57 ± 1	57 ± 3
k_0	0.92 ± 0.01	NA
ξ^2 / ν	0.4	0.1

2. Testing of the Circuit at High-Voltage

The testing mentioned previously was performed at values of V_{Ch} < 1,100 V. Additional tests of the circuit at higher voltages were done to test the reliability of the thyristor and diode, and some of the high-voltage insulation. After re-installing the diode in the switch-assembly, the acceleration coil-circuit was tested at values of V_{Ch} up to about 3,000 V (at the high end of the range, the charge voltage was not known precisely, as the voltage probe has a limit of 2,200 V). Fig. 9.a. shows current waveforms for V_{Ch} < 1,900 V. The trigger pulse to the thyristor gate driver circuit was applied at t = 0 s. The diode does indeed shut off the thyristor after the first half-cycle, although there is some overshoot, which increases with increasing V_{Ch}.

A key parameter for the diode is its reverse recovery charge, Q_{rr}, which is roughly the amount of charge that flows in the direction opposite to that of the initial discharge current before the current reversal is blocked. For the diode used the value of Q_{rr} was 1.8 mC. Considering the fourth curve in Fig. 9. (V_{Ch} = 1,827 V), the total charge transferred during current shut-down, i.e. between the zero-crossing in the current and the point where the current finally goes to zero, is ΔQ = 4 mC, over twice as large as Q_{rr}. When V_{Ch} was increased further to about 2,000 V, the

diode failed as a short, although with some finite resistance. After the diode failure, the current wave-forms were those of a damped ringing circuit, as seen in Fig. 9.b.

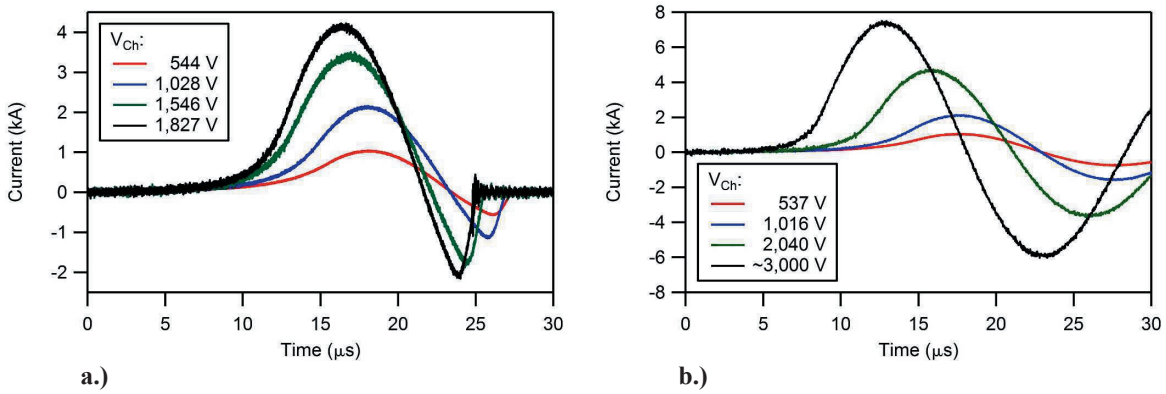

Figure 9. Current waveforms for the unloaded acceleration-coil circuit: a.) Before failure of the diode, and b.) after failure of the diode.

For the maximum value of V_{Ch} ~ 3,000 V, the peak current reached was 7.4 kA. Defining a characteristic switch delay time, t_D, as the time between receipt of the trigger signal by the gate circuit and the time when the current reaches 10% of its peak value, the delay time was found to be $t_D = (9.6 \pm 0.2)$ μs, at least for values of V_{Ch} * 2,100 V. At higher voltages (V_{Ch} ~ 3,000 V) the delay appears to be shorter, $t_D = 7.3$ μs in this case, although there was not enough data at these voltages to conclusively determine a trend.

The values of total circuit inductance and resistance were calculated for all cases. The calculations of L_{circ} yielded the same results as found above for the unloaded coil. The calculated resistance, R, as a function of V_{Ch} is shown in Fig. 10. The resistance decreases with increasing V_{Ch} and so also with increasing current, and it appears to reach an asymptotic value at 3,000 V or higher. This trend indicates that a significant source of resistance lies in the thyristor itself. The circuit resistance is higher after the diode failure than before, although it exhibits the same decreasing trend. The lowest resistance measured (at V_{Ch} ~ 2,000 V) was 38 mς. It is possible that the pressure applied by the clamp assembly relieved over time, and that re-torquing it would reduce the resistance some. It may also be possible to significantly reduce the resistance further with more and/or larger conductor cables.

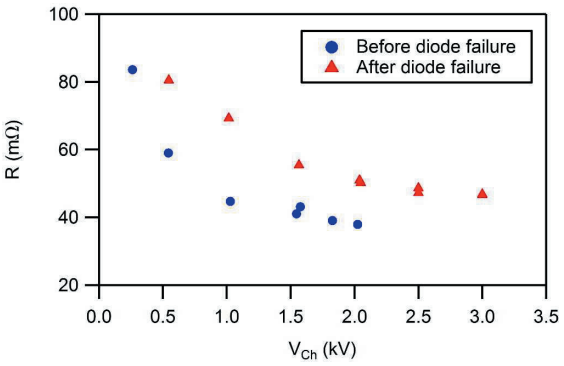

Figure 10. Circuit resistance, *R*, as a function of V_{Ch}.

B. Vacuum Testing

After bench-top testing was completed, the RTV high-voltage insulation was applied to the acceleration coil and the switch assembly, as described in sections II.A. and II.C., and the thruster was reassembled with all its components. Finally, the finishing insulation was applied to the remaining exposed metal surfaces. The completed thruster, shown in Fig. 11, was placed in a 2.19 m long by 1.05 m diameter vacuum chamber for testing (total volume of 1.9 m^3); although the pumping speed for this chamber is relatively low, it was deemed acceptable for cyclic operation up to ten to twenty pulses. The propellant gas used for these tests was argon. The run-tank described in section II.D. was not used for these tests, rather the gas was sourced from a bottle outside the vacuum chamber. Consequently, the mass-bit could not be determined precisely, but based on previous testing of the pulsed gas-valve, it is estimated to be about 25 μg / pulse for cyclic operation.

The capacitor bank was charged with a General Atomics CCS high charge-rate power-supply; the power-supply and charge system are described in some detail in reference 4. The charge wires were silicone rubber high-voltage cables, connected to the thruster through a vacuum feed-through. Both the pre-ionizer circuit and the thyristor gate circuit were located outside the chamber and were connected to the thruster through vacuum feed-throughs.

The pre-ionizer system was tested first; the capacitor was left uncharged and only the gas-valve and pre-ionizer circuit were turned on. Operating in single-shot mode, the gas-valve was commanded open and a dim but distinct purple flash of light was observed over the coil face. An image of the thruster in the vacuum chamber and a time-integrated image of the discharge, extracted from video of the test, is shown in Figs. 12.a. and b. respectively. The glow appears to be brightest in the region of the pre-ionizer inner-electrode. Cyclic operation of the pulsed gas valve and pre-ionizer was demonstrated at a rate of 1 Hz for several pulses.

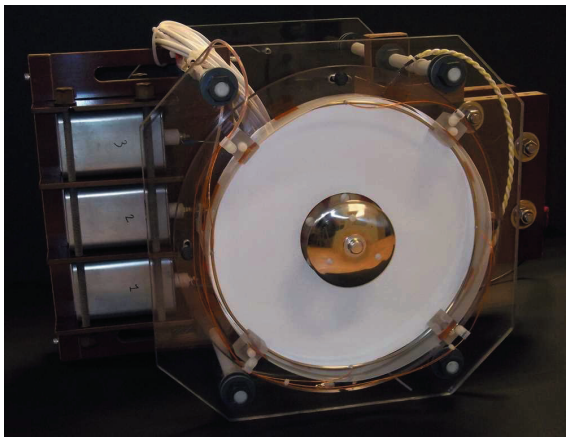

Figure 11. The completed thruster ready for installation in the vacuum chamber.

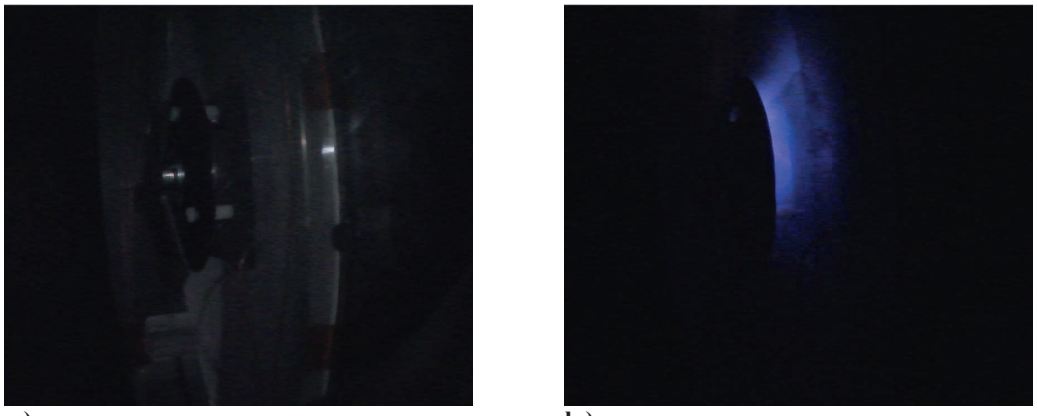

a.) **b.)**

Figure 12. Single-pulse operation of the pre-ionizer: a.) the coil face as viewed through a vacuum port. b.) a plasma is formed when gas is injected by the valve.

The thruster was then operated in single-pulse mode with the capacitor bank charged to 2 kV. Higher voltages were not attempted, so as to not overtax the insulation during these initial tests. Time-integrated pictures (again, extracted from video) of a single-pulse discharge are shown in Fig. 13. The character of these discharges was markedly different than with the pre-ionizer alone; a bright bluish-white glow was seen over the coil-face, and the plasma seemed to form a broad jet, emanating from the coil and bounded by the propellant cuff. It was also found that the acceleration coil circuit was able to form a plasma by itself, without use of the pre-ionizer. These discharges were also relatively bright, though perhaps not as bright as with the pre-ionizer. It is not possible to do more than note the apparent qualitative difference at this time; conclusions about any difference in operation of the device with and with-out the pre-ionizer will require quantitative measurements that have yet to be performed.

The thruster was also run repetitively for up to 12 pulses at a cyclic rate of 2 Hz. Operation at higher cyclic rates was attempted, but could not be achieved. Both the thyristor gate-driver circuit and the pulsed gas valve had previously been individually tested at cyclic rates up to 20 Hz, and found to operate without difficulty at those speeds. It was determined that the limitation in cyclic rate was due to the valve being starved of gas, likely from debris clogging the inlet.

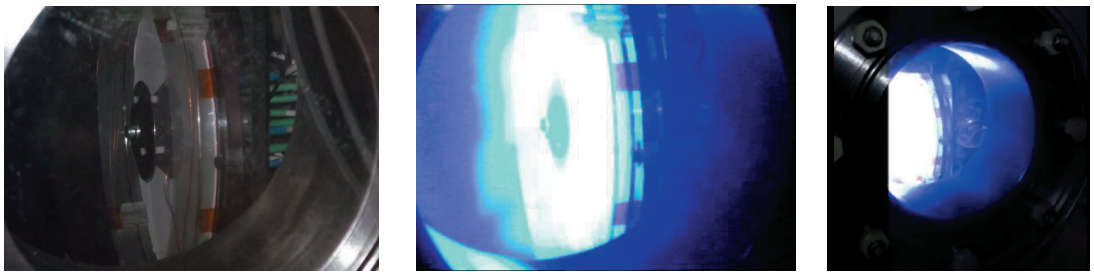

a.) b.) c.)

Figure 13. Operation of the IPPT: a.) A view of the thruster in the vacuum chamber. b.) The plasma formed over the coil face during a single-pulse discharge with V_{Ch} = 2 kV. c.) Another single-pulse discharge showing a plasma jet originating at the coil-face.

When operated for more than 15 pulses or so, the region behind the coil would start lighting up, indicating that plasma was forming there. Soon thereafter, arcing would occur shorting the connections to the power-supply. Subsequent inspection of the thruster revealed two locations where arcs had punched through the insulation and charred it: on the positive terminal of the capacitor and on the anode of the thyristor. The location of the insulation failures indicates that plasma behind the coil permitted a low-inductance current path that bypassed the coil. Even after these events however, the capacitor and thyristor still worked and, once the chamber was evacuated, the thruster could be operated again. No insulation failures were found in the acceleration coil or on any of the high-voltage cables.

IV. Conclusion

A. Conclusions

A few conclusions, based on this initial testing of the thruster, are summarized as follows:

- The inferred external inductance of 336 nH, a little less than half that of the acceleration coil itself, was lower than expected. The use of bundled high-voltage cables appears to be a practical method for making the connections between components, without introducing too much stray inductance.
- The thyristor proved to be suitably robust for testing purposes in these initial tests. Although, to date, we have stayed well below its maximum operating voltage, the currents that the switch has carried have been in excess of its rated RMS value.
- The series fast recovery diode functioned more-or-less as desired in interrupting the current flow after the first half-cycle of the discharge at charge voltages up to about 2 kV. In a thruster, it might be practical to gang several such diodes in parallel, although this would require a balancing network that would subsequently introduce some resistance into the circuit. If the diodes used were selected so as to have very similar I-V characteristics, this added resistance might be acceptably low. Alternatively, some other kind of solid state switch might be used to block the reverse current, such as a gate turn-off thyristor (GTO), or an IGBT.
- The glow-discharge pre-ionizer worked within the limited scope of the tests conducted. Moreover, it was found that, even at the relatively low voltages used, the dI/dt of the acceleration coil current itself was sufficient to ionize the propellant. Further testing will be required to determine if this pre-ionizer concept is practical and provides a measureable improvement in the thruster's performance.

B. Future Work

The immediate plans for continued work on this device are to rework the insulation of the capacitor and switch assembly so as to preclude arcing to these components. Also, the pulsed gas-valve will be cleaned and rebuilt and a filter included in the propellant line, so as to permit operation at cyclic-rates up to 30 Hz. The run-tank, mounted on the thruster itself will also be used. Following that, the thruster will be tested again on a thrust-stand in a large, high-throughput vacuum chamber. Testing of the thruster with another valve, that is being developed as part of an independent research effort to develop a fast, reliable pulsed-gas valves for IPPTs, will also be conducted.

Acknowledgments

The authors thank Jim Martin, Patrick McRight, Tom Williams, and Mary Beth Koelbl of the Marshall Space Flight Center (MSFC) Propulsion Systems Department and Mike LaPointe of the MSFC Technology Development and Transfer Office for continued management support and encouragement of this work. We also thank Emeritus Professor Ralph Lovberg (University of California San Diego) and Ashley Hallock (OHB Sweden AB) for many useful discussions about IPPTs. This work was in-part sponsored by the In-Space Propulsion Project of the Game-Changing Development (GCD) Program of NASA's Office of the Chief Technologist. The GCD principle investigator was Chuck Taylor (NASA Langley Research Center) and the project manager was Tim Smith (NASA Glenn Research Center).

References

[1]Polzin, K.A., "Comprehensive Review of Planar Pulsed Inductive Plasma Thruster Research and Technology," *Journal of Propulsion and Power*, Vol. 27, No. 3, 2011, pp. 513-531.

[2]Dailey, C.L., Lovberg, R.H., "The PIT MkV Pulsed Inductive Thruster", *TRW Systems Group*, NASA CR-191155, 1993.

[3]Dankanich, J.W., Polzin, K.A., "Mission Assessment of the Faraday Accelerator with Radio-Frequency Assisted Discharge (FARAD)," *44th AIAA/SAE/ASME/ASEE Joint Propulsion Conference, Hartford, CT*, AIAA-2008-4517, 2008.

[4]Polzin, K.A. et al., "Summary of the 2012 Inductive Pulsed Plasma Thruster Development and Testing Program", *Marshall Space Flight Center*, NASA TP-2013-217488, 2013.

[5]Toftul, A., Polzin, K.A., Martin, A.K, Hudgins, J.L., "Testing of Diode-Clamping in an Inductive Pulsed Plasma Thruster Circuit," *50th AIAA/SAE/ASME/ASEE Joint Propulsion Conference, Cleveland, OH*, AIAA-2014-3503, 2014.

[6]Polzin, K. A., "Scaling and Systems Considerations in Pulsed Inductive Plasma Thrusters," *IEEE Transactions on Plasma Science*, Vol. 36, No. 5, 2008, pp. 2189-2198.

[7]Martin, A. K., Eskridge, R.H., "Electrical coupling efficiency of inductive plasma accelerators," *Journal of Physics D: Applied Physics*, Vol. 38, Dec. 2005, pp. 4168-4179.